

Mechanical behaviour evaluation of adhesively bonded joints of aircraft structures

Sérgio Nunes Correia
sergio.n.correia@tecnico.ulisboa.pt

Instituto Superior Técnico, Lisboa, Portugal

October 2016

Abstract

The structural integrity of some structures can be related to the strength of their unions. Over the years, adhesively bonded joints have been often chosen over several mechanical systems based joints, as welding or riveting. Among others, the reduction in stress concentrations, the ability of producing smooth surfaces, with no discontinuities and the reduced weight penalties are some of the factors that make this type of joints so attractive. However, when compared with these other joining techniques, it can be verified that there are practically no accepted guidelines for predicting the strength of an adhesive joint, being the design of some joints still based in personal experience and in the so-called rules of thumb. Recently, some numerical models have been proposed to estimate the failure load of bonded joints. The main problem is related with the fact that, for most of these methods to be applied, some experimental tests must be performed to identify some material models, which is not always convenient. With this in mind, an experimental study was performed, based in the Single Lap Joint from the ASTM D 1002 standard method, with the objective of determining the best surface treatment, for aluminum-to-aluminum joints, using two types of adhesives. Furthermore, a computational model, using the Finite Element Method, has been implement in order to predict the adhesive behavior, taking only the stress-strain curve of the adhesive as an input.

Keywords: Adhesive, Adhesively Bonded Joint, Single Lap Joint, Surface Treatment, ASTM D 1002, FEM

1. Introduction

With the advances in manufacturing techniques, several improvements have been verified in structural adhesives. As a direct result of this improvements, the use of bonded joints has supplemented or replaced the use of mechanical-based joints in several aeronautical structures. Between other advantages, adhesively bonded joints allow a better load distribution, increase in the service life, reduced machining cost and reduced complexity [1].

Despite the many advantages, bonded joints also suffer from a significant number of limitations. Among others, one can identify the bad adhesion to some substrates, weak resistance to cleavage stresses or the degradation due to exposure to hostile environments [2]. However, in contrast to more conventional joining techniques, the major concern related with adhesively bonded joints is that there exist practically no generally accepted guidelines to predict the joint strength. The aerospace industry, which has been developing the technology, is still designing joints mainly based in previous experi-

ence and rules of thumb.

Recently, some computational methods have been developed to modulate adhesively bonded joints. Nonetheless, most of these methods are based in damage mechanics, meaning that several experimental tests need to be performed in order to enquire about the damage models of the adhesive. In this way, the development of simple and accurate techniques to predict the failure of this type of joints, with the minimum number of experimental tests, would be a great improvement to the industry.

Several studies and analysis show that the bond strength of an adhesively bonded joint depends on many factors, such as the bonded area, the environment in which the structure will be used, the service temperature, the type of surface treatment applied to the adherents and, of course, the type of adhesive used. With all this in mind, it is easy to see that all these factors are strictly related to aircraft security, meaning that a very thoughtful joint design and adhesive choice are essential.

Said so, the main motivation of performing this work is, firstly, to study and experimentally evaluate the behavior of adhesively bonded joints when subjected to different types of surface treatments and when bonded with different adhesives, specially in terms of adherence. Secondly, it is of great interest to develop a computational model capable of predicting the failure of a bonded joint, assuming perfect conditions of adhesion between adhesive and adherents and having only as information the stress-strain curve of the adhesive.

This work has been developed in cooperation with TAP Maintenance & Engineering (TAP M&E). Actually, the adhesive used to repair the engine nacelle structure is being discontinued. In this way, knowing about the possibility of performing some types of anodizing in their complex, TAP M&E engineers are trying to find a combination of a new adhesive and surface treatment, that can be performed indoors and ensure a joint strength at least as good as the old one.

With this in mind, two principal objectives are proposed in this work, being one experimental and the other numerical. These are:

- Identify, experimentally, an optimum combination of adhesive and surface treatment that can be performed inside TAP M&E complex.
- Develop a computational model that can predict the behavior and strength of bonded joints.

The Single Lap Joint (SLJ), present in Figure 1, is the type of bonded joint most used in an aircraft, specially due to the ease of produce, inspect and repair [3]. Said so, this work will be oriented to the study of the SLJ.

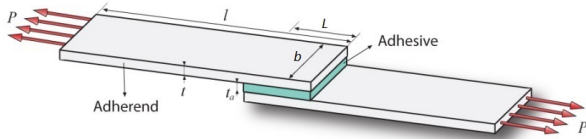


Figure 1: Single Lap Joint [3].

2. Literature Review

2.1. Analytical Methods

Starting to analyze the SLJ, a project parameter can be defined. This parameter is the apparent shear stress, $\bar{\tau}$, present in the adhesive layer, and is given by Equation 1.

$$\bar{\tau} = \frac{P}{bL} \quad (1)$$

Where P represents the applied load, b the SLJ width and L the bond overlap.

Due to the fact that adhesives are not rigid, non uniform strain is verified across the bondline, developing, consequently, a non uniform shear stress distribution. Moreover, since the loads are not initially in the same line of action, a bending moment will be developed in the joint, leading to the development of peel stresses in the adhesive layer.

Over the years, several methods have been developed to solve, analytically, both these shear and peel stress distributions. The first analytical method to solve the SLJ stress distribution was developed by Volkersen [4], in 1938. Volkersen was the first to consider the non uniform strain in the bondline. Despite, this method presents some limitations, related with the fact that the bending moment effects were neglected. Only an expression for the shear stress distribution was obtained, being presented in Equation 2, for equal adherents. λ is given by Equation 3. The adhesive was considered perfectly elastic.

$$\tau(x) = \frac{P\lambda}{2} \left[\frac{\cosh \lambda x}{\sinh \lambda \frac{L}{2}} \right] \quad (2)$$

$$\lambda = \sqrt{\frac{2G_a}{Et_a t}} \quad (3)$$

Where P is the applied load, E is the adherent elastic modulus, t represents the adherent thickness and G is the elastic shear modulus. When accompanied by a subscript a , the parameters are referent to the adhesive.

In 1944, Goland and Reissner [5] were the first to consider the effects related with the bending and transverse force that occurs due to the non-collinearity of the applied load. The solution for the shear stress distribution is given by Equation 4, being k the bending moment factor.

$$\tau(x) = \frac{P}{8c} \left[(1 + 3k)\delta \frac{\cosh \frac{\delta x}{c}}{\sinh \delta} + 3(1 - k) \right] \quad (4)$$

The expression to the bending moment factor, k , is presented in Equation 5, being u_2 given by Equation 6.

$$k = \frac{\cosh u_2 c}{\cosh u_2 c + 2\sqrt{2} \sinh u_2 c} \quad (5)$$

$$u_2 = \sqrt{\frac{3(1 - \nu^2)}{2}} \frac{1}{t} \sqrt{\frac{P}{t^2 E}} \quad (6)$$

For the peel stress, the expression is given in Equation 7.

$$\begin{aligned} \sigma(x) = \frac{Pt}{\Delta c^2} & \left[\left(R_2 \lambda^2 \frac{k}{2} + \lambda k' \cosh \lambda \cos \lambda \right) \times \right. \\ & \times \cosh \left(\frac{\lambda x}{c} \right) \cos \left(\frac{\lambda x}{c} \right) + \\ & + \left(R_1 \lambda^2 \frac{k}{2} + \lambda k' \sinh \lambda \sin \lambda \right) \times \\ & \left. \times \sinh \left(\frac{\lambda x}{c} \right) \sin \left(\frac{\lambda x}{c} \right) \right] \end{aligned} \quad (7)$$

The parameters of the peel stress distribution equation are given in Equations 8.

$$\lambda = \left(\frac{6E_a c^4}{t_a E t^3} \right)^{0.25} \quad (8a)$$

$$k' = \frac{kc}{t} \sqrt{3(1-\nu^2) \frac{P}{E}} \quad (8b)$$

$$R_1 = \cosh \lambda \sin \lambda + \sinh \lambda \cos \lambda \quad (8c)$$

$$R_2 = \sinh \lambda \cos \lambda - \cosh \lambda \sin \lambda \quad (8d)$$

$$\Delta = \frac{1}{2} [\sin 2\lambda + \sinh 2\lambda] \quad (8e)$$

As well as Volkersen, Goland and Reissner considered the adhesive as perfectly elastic.

Hart-Smith [6], in 1973, was the first to consider the plastic deformation in the adhesive, in addition to the elastic response. If the adhesive plasticity is allowed, the analytical joint strength prediction will be higher, since a failure strain criteria can be used instead of a stress based criteria.

To characterise the adhesive behaviour, Hart-Smith used an elastic-perfectly plastic model - Figure 2.

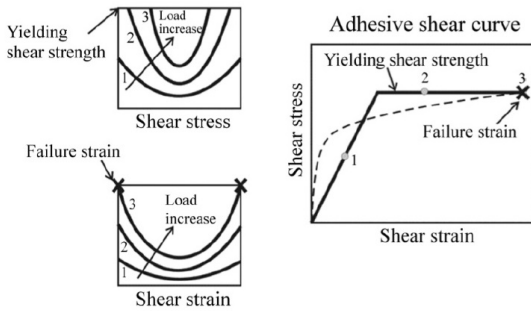


Figure 2: Effect of plasticity in the adhesive layer according to Hart-Smith [6].

In Figure 2, there are three different cases, that are obtained by increasing the applied load, P . In short, for Case 1 the adhesive is in the elastic range. For Case 2, the adhesive starts to yield, since the yield limit has been overcome. Finally, for Case 3, the adhesive fails, due to the fact that the shear strain achieves its ultimate value.

Hart-Smith developed two solutions for the peel and shear stress distributions: the first one, assuming a purely elastic model and, as previously referred, a second one using an elastic-perfectly plastic model.

For the first solution, distributions are presented in Equations 9 and 10, for shear and peel stresses, respectively. The equations are valid for equal adherents.

$$\tau(s) = A_2 \cosh 2\lambda' s \quad (9)$$

$$\sigma_c(s) = A \cos \chi s \cosh \chi s + B \sin \chi s \sinh \chi s \quad (10)$$

Where $-c \leq s \leq c$. Constants A_2 , A and B are obtained using Equations 11.

$$A_2 2\lambda' \sinh 2\lambda' c = \frac{G}{E t t_a} \left[P + \frac{6(1-\nu^2)M_0}{k_b t} \right] \quad (11a)$$

$$A = -\frac{E_c M_0 [\sin \chi c - \cos \chi c]}{t_a D \chi^2 e^{\chi c}} \quad (11b)$$

$$B = \frac{E_c M_0 [\sin \chi c + \cos \chi c]}{t_a D \chi^2 e^{\chi c}} \quad (11c)$$

Considering the plasticity, the shear stress distribution is given by Equation 12. Also, the solution for the shear strain distribution is presented in Equation 13. The origin for ζ is defined at $s = d/2$, being only valid in the range $[d/2, c]$. d represents the length of the elastic range.

$$\tau = A_2 \cosh 2\lambda' s + C_2 \quad (12)$$

$$\gamma = A_3 \zeta^2 + B_3 \zeta + C_3 \quad (13)$$

The constants A_2 , B_2 , A_3 , B_3 and C_3 , as well as the unknown ratio d/l are found by solving a system of equations that arises from the application of the BC defined.

2.2. Numerical Analysis - The Finite Element Method

The use of the Finite Element Method (FEM) to study the behavior of bonded joints has been quite used in the academic world, specially due to the great number of commercial software available and their ease of use. The computational analysis developed during this work were all performed using ANSYS Parametric Design Language (APDL). The version of the software used is ANSYS 14.0.

As well as in every finite element (FE) software, there are several essential parameters that will influence the quality and accuracy of the results. Among others, should be emphasized the type of FE used and the mesh density (MD) [7]. One typical choice

for adhesively bonded joints are continuum solid elements, suited for non-linear problems involving plasticity and large deformations. Regarding the MD, it do not need to be equally refined across all the geometry. Due to the complex stress state present in the adhesive layer, a more refined mesh is recommended in this location [8].

A 2D analysis in plane strain conditions is almost preferred for the most authors [9, 10] and will be adopted during the development of this work.

The FEM presents two main problems when applied in the analysis of bonded joints: first, the adherents are too big when compared with the very thin adhesive layer, which can cause mesh problems and very slow models. Second, if the non-filleted geometry of the adhesive is considered, singularities appear in the perfectly sharp corners of the bonded joint.

As stated by Yue and Wahab [11], a stress singularity is detected by divergence of peak stress with the mesh refinement. The most common way of handling this problem is to use the stresses obtained along the center-line of the adhesive, being the convergence in these points achieved for a certain mesh density. This method is defined as the Centerline Method and can be used to compare computational results with the classical solutions. However, a problem arises from this simplification: the stresses used are average stresses, not representing the variation of shear and peel stresses across the adhesive thickness.

The other way of handling singularities implies changing the geometry of the SLJ. In practice, the adherent corners are not perfectly sharp, so a small rounding can be added (Figure 3). Also, during bonding, there is always some adhesive that flows to the sides, creating a small fillet. Several researchers even state that the fillet is essential to obtain accurate results, advising that it shall be built, with an extra piece of adhesive, during the specimen manufacturing. Combined with the rounding, the fillet modulation prevents the appearance of strong singularities during the analysis.

Regarding the failure load calculation, the first step consists in defining an appropriate and effective method for the analysis to be performed.

The most common method to evaluate material failure is using continuum mechanics. Essentially, approaches based on continuum mechanics use the maximum values of stress or strain distributions against a chosen failure criterion, which uses the critical values of the material. Some advantages related with this kind of methods are the simplicity of use and the fact that little information is needed for the criteria, due to the dependency on one or few parameters.

This method presents a great limitation, which

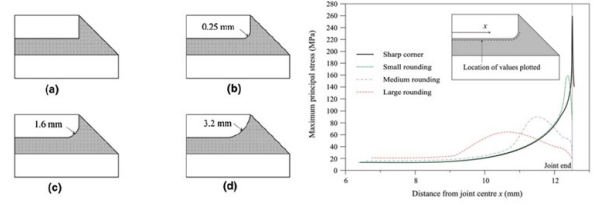


Figure 3: On the left, singular point D of the SLJ with different degrees of rounding: a) sharp corner; b) small rounding; c) medium rounding; d) large rounding (please note that the thickness of the adherent, in this Figure, is 3.2 mm). On the right, shear stress distribution for each of the cases. [12].

is the assumption that the structure fails as soon as the failure criteria is verified at some point, i.e., it assumes that the material presents a very brittle behavior. This is not always true, specially when analyzing very ductile materials, like adhesives [13].

Some other methods have been proposed in recent years, like the Cohesive Zone Modelling (CZM). However, to be applicable, more experimental tests than the bulk test are necessary, which is not always convenient [13, 14, 15, 16]. Also, some of the models consists in changing the input parameters based in experimental observations. This still demands the realization of experimental tests, which is what one wants to avoid.

A new method has been arising lately, being based in the local application of a continuum mechanics failure criterion. This method is named Progressive Failure Method (PFM) and has been widely used in the past few years to calculate the failure load of composite materials, with a very good degree of success [17, 18, 19, 20]. More recently, this method started to be implemented in the analysis of some adhesive joints [2, 21].

Essentially, the PFM involves three main stages that act in a cyclic way, being them the stress and strain analysis, the failure analysis, using an appropriate failure criterion and, finally, the application of the material degradation rule to the failed elements.

To better understand how the analysis is performed, a flowchart of the code is highlighted in Figure 4.

Some good results have been obtained with the PFM [21, 2]. In addition of predicting the failure load, the PFM also allows to make a prediction of the failure path.

2.3. Adherence and Types of Failure

All the considerations presented in Subsections 2.1 and 2.2 were made assuming a perfect adherence between the adhesive and adherents, with the failure occurring in the adhesive layer. However, in real

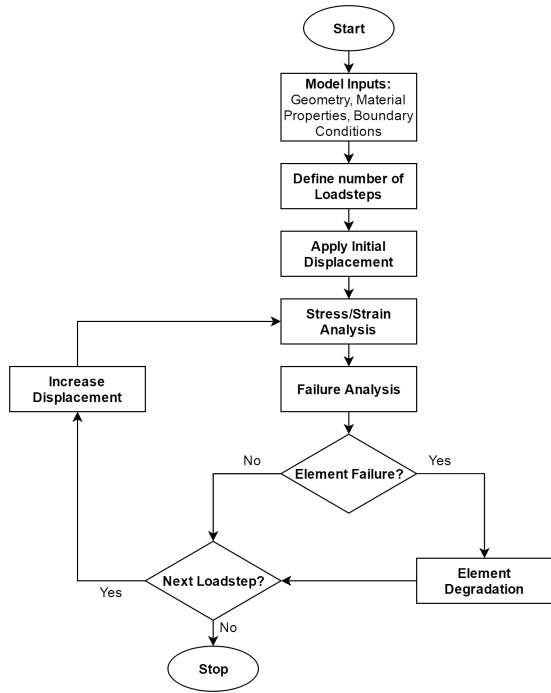


Figure 4: Flowchart for the Progressive Failure Model, adapted from [21].

joints, this is not always the case and four types of failure modes can be identified (Figure 5), being them [22]:

- Cohesive Failure - it is characterized by failure of the adhesive itself;
- Adhesive Failure it is characterized by a failure of the joint at the adhesive/adherent interface and is typically caused by inadequate surface preparation, chemically and/or mechanically;
- Adhesive-Cohesive Failure - the failure presents the previous two types simultaneously;
- Adherent failure - it is characterized by failure of the adherent instead of the adhesive. In metals, this occurs when the adherent yields.

Adhesive failures are intimately related with two main factors: the surface treatment of the adherents and the use of primers or adhesion promoters.

A surface treatment is applied in a material to provide the best possible bonding conditions. There are several types of surface treatments for metals which can be classified as either micro-mechanical, macro-mechanical, chemical or a combination of these [23]. In this work, only chemical surface treatments will be tested, being them the Phosphoric Acid Anodyzing (PAA), the Chromic Acid Anodyzing (CAA), the Sulfuric Acid Anodyzing (SAA) and the Boric-Sulfuric Acid Anodyzing (BSAA) [24]. The first two types are the treatments advised in the

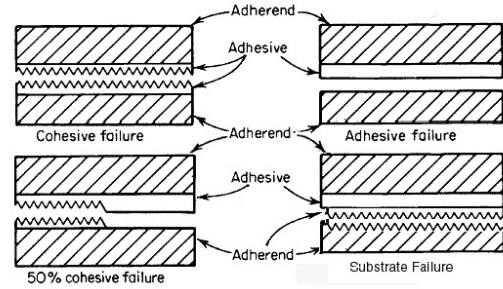


Figure 5: Failure types in a bonded joint: cohesive failure on the top left; adhesive failure on the top right; adhesive-cohesive failure on the bottom left; adherent failure on the bottom right [22].

adhesive's data-sheets, while the last two are the ones that can be performed in TAP M&E complex.

When the surface treatments are not so efficient, adhesion and permanence time can be increased by primers or adhesion promoters [25]. These type of materials work in a similar way to improve adhesion, adding a new, usually organic, layer at the interface between adhesive and substrate.

3. Methods and Materials

3.1. Methods

As stated, the SLJ will be the main focus of this work. The usual test for this type of joints is the ASTM D 1002 [26], consisting essentially in the steps described.

- The specimen must be placed in the grips of the testing machine.;
- The load shall be applied immediately to the specimen. The crosshead speed must be 1.3 mm/min;
- Apply the load to failure.

The overlap used and the geometry of the specimen can be seen in Figure 6. The thickness of the metal, t , is 1.6 mm, being the adhesive thickness dependent on the type of adhesive used.

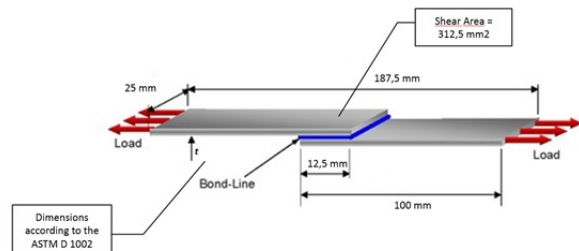


Figure 6: SLJ Specimen geometry.

From the realization of this test, one obtain the failure load of the joint, P_f . To obtain the apparent failure shear stress from P_f , Equation 1 can be used

3.2. Materials

The only adherent tested is the aluminum 2024-T3 alloy. Since the main interest of the work is to study the adhesive behavior, one must guarantee that the adherents are in the elastic region. This was verified using a simple analytical method proposed by Adams and Wake [1].

Regarding the adhesives, two types were tested in this work: the Henkel Loctite EA 9658 Aero and the 3M Scotch-Weld AF 163-2. Both are considered structural adhesives, manufactured in film form and widely used in the aerospace industry. These two adhesives are tested in order to replace an old one - the Hysol EA 9689, also produced by Henkel Loctite.

Also, each adhesive is advised to be used with a primer, in order to improve their adherence to the substrates. The Scotch-Weld EC-3924B must be used with the adhesive AF 163-2, while Henkel Loctite EA 9258.1 AERO is advised to be used along with the EA 9658 AERO adhesive.

Due to the impossibility of performing the bulk tensile tests to determine the stress-strain curves of both adhesives, this properties were obtained following the work done by de Freitas and Sinke [27], for the AF 163-2. For the EA 9658 AERO, the mechanical properties of a similar adhesive were used. The adhesive chosen had a similar apparent failure shear stress and had the same curing and storage conditions. Plus, both are designed to metal and honeycomb bonding, indicated that it might be a good approximation.

With the analysis of de Freitas and Sinke [27] work and following the formulation presented by Hart-Smith [6], the adhesives were modelled as elastic-perfectly plastic.

All the mechanical properties used are presented in Table 1.

Table 1: Resume of the properties used.

Parameter	AF 163-2	EA 9658	2024-T3
E [GPa]	2.04	2.62	72.40
ν	0.34	0.34	0.33
σ_y [MPa]	45.70	56.00	347.00
ε_y [%]	2.24	2.14	-
ε_p [%]	5.38	6.00	-
G [GPa]	0.76	0.98	-
τ_y [MPa]	26.38	32.33	-
γ_y [%]	3.88	3.71	-
γ_p [%]	9.32	10.39	-
$\bar{\tau}_f$ [MPa]	39.30	40.00	-
t [mm]	0.24	0.60	1.60

3.3. Specimens Manufacturing

The specimens used in the experimental tests were built in TAP M&E facilities. The manufacturing process had two main phases: Surface Treatment and Bonding.

To apply the Surface Treatment, it is necessary to firstly clean the adherents surface. This is essential to remove any type of grease or impurity from the aluminum. Immediately after, the aluminum is activated by acid action, being submerged in a bath that promotes the creation of micro-pores in the surface. Next, the plates are submerged in an anodize solution bath for 45 minutes, at a temperature between the 24 and 29 °C, with a direct current applied on them of 15 V. The electric current passing through the anodize solution converts the aluminum surface in a form of oxide, increasing the contact area. Finally, a surface finish is applied. This process is used typically to increase corrosion resistance and promote, even more, adherence of paints and adhesives.

For both adhesives, the process of bonding is quite similar, being described next. All the process was performed in a clean room, under controlled environment.

Regarding the Bonding phase, it starts with the application of the respective primer and cure. After curing, the adhesive can be applied in the desired area. To prevent the stress concentrations, and to obtain more reliable results, an adhesive fillet is added manually to each side of the bond layer. Finally, the adhesive is cured. The specimens are inserted inside a peel-ply bag in order to create a vacuum environment. The cure method was different for each adhesive. Due to the high cure temperature, the EA 9658 AERO specimens were cured with thermal blankets, while the AF 163-2 specimens were cured in the drying oven.

3.4. Number and type of specimens

Two types of SLJ were tested, one representing a new joint (NJ), while the other was representing a repaired joint (RJ). The surfaces of the adherents were different in the RJ: one substrate was prepared with a type of anodizing, while the other was completely clean, without any kind of treatment. Both types of joints were combined with the two adhesives, as well as with the two types of anodizing. The ASTM D 1002 advices to perform at least 5 tests for each type of specimen studied. To increase the reliability of the results, 7 tests were conducted for each one. Altogether, 56 tests were performed. In Table 2 are presented all the combinations used.

4. Results and Discussion

The results have been divided in three main subsections: analytical results, experimental results and computational results. To simplify the reading,

Table 2: Tests performed for each specimen.

Adhesive	Treatment	Joint Type	
		NJ	RJ
AF 163-2	BSAA	7	7
AF 163-2	SAA	7	7
EA 9658 AERO	BSAA	7	7
EA 9658 AERO	SAA	7	7

when conclusions are identical for both adhesives, graphical plots are only presented for the AF 163-2. Numerical values will be presented for both adhesives.

4.1. Analytical Results

A theoretical analysis of the SLJ was the first step of this work. Using the classical solutions presented, with an applied load of 6000 N, the distributions presented in Figure 7 are obtained. The curves are quite similar for the EA 9658 AERO, exception made for the plasticized area, which is lower.

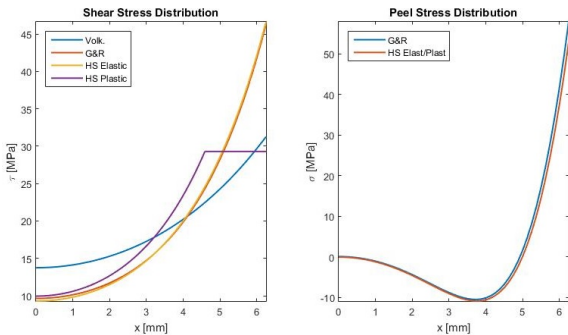


Figure 7: Shear and Peel Stress distributions for the AF 163-2 adhesive.

Analyzing Figure 7, one can see that Volkersen solution is clearly different from the other two, due to the non consideration of the bending moment in the joint. Furthermore, as stated, the peel and shear peaks occur in the borders of the adhesive, not satisfying the shear stress free boundary condition [28]. Also, When the adhesive is assumed elastic-perfectly plastic, Hart-Smith method shows how the adhesive borders start to plasticize in shear.

With these distributions, a first estimation of the failure load can be obtained. These values are calculated using an incremental load approach, combined with an adequate failure criteria. Essentially, a maximum shear or peel stress criterion was chosen for all the classical solutions, except for the plastic formulation of Hart-Smith, where a maximum shear strain was selected. In addition, specially due to its simplicity, the failure load obtained by the Limit State Analysis is also calculated for each adhesive [29].

The results obtained are presented in Table 3. The errors are relative to the data-sheets values given in Table 1.

Table 3: Relative error for each solution.

Solution	AF 163-2		EA 9658 AERO	
	P_f [N]	ϵ_{rel} [%]	P_f [N]	ϵ_{rel} [%]
Volk	5622	54.22	8513	31.90
GR	3677	70.06	6207	50.34
HS (Elast)	3627	70.47	5826	53.39
HS (Plast)	6957	43.35	11962	4.30
LSA	9153	25.47	11422	8.62

Most of these predictions present really high relative errors, specially all the values obtained using the perfectly elastic classical solutions. The plastic formulation proposed by HS is much more accurate than the other classical solutions, due to the aforementioned consideration of the adhesive plasticity. Also, despite the simplicity, the LSA proved to be a method with a very good accuracy. In fact, for the EA 9658 AERO adhesive, the relative error is only 8.62 %.

4.2. Experimental Results

Prior to the tests, measures to the adhesive thickness and fillet length must be performed for each specimen - Table 4. This values are quite important model computationally the geometry of the SLJ As it can be seen, there are some differences between the theoretical and measured thickness values, which could lead to errors.

Table 4: Average measures of t_a and l_{fil}

Adhesive	t_a [mm]	l_{fil} [mm]
EA 9658 AERO	0.425 ± 0.045	7.082 ± 0.913
AF 163-2	0.263 ± 0.053	7.468 ± 0.911

The results obtained, for the apparent failure shear load of each specimen, are presented in Figure 8.

Analyzing Figure 8, it is clear that, when applied to NJ specimens, the AF 163-2 presents a better mechanical behavior when compared with the EA 9658 AERO. The best results are obtained for the SAA NJ, bonded with the mentioned AF 163-2, with a value of $\bar{\tau}_f = 24.96$ MPa. This value represents an improvement of 8% relatively to the old adhesive, meaning that the goal of finding a solution at least as good as the old one was achieved.

However, when applied to RJ, the mechanical behavior of the AF 163-2 is really bad, being surpassed by the EA 9658 AERO. Even so, due to the fact that this kind of test was not performed by the manufacturer, it is impossible to infer if the EA 9658 AERO

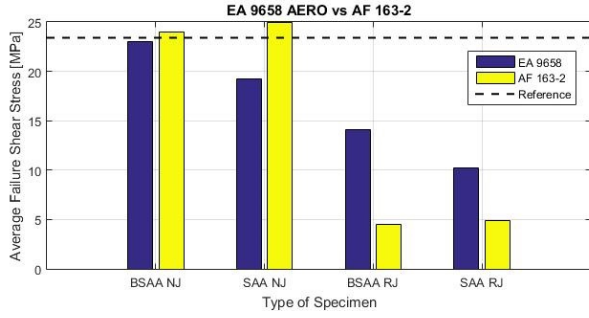


Figure 8: Apparent failure shear stress for both adhesives.

brings any kind of improvement in bonding RJ relatively to the Hysol EA 9689. Furthermore, due to the low values obtained, the security of a repaired joint cannot be guarantee, and further tests shall be performed.

4.3. Computational Results

For the computational analysis, the FEM was used. The type of FE chosen was the PLANE82, defined by by eight nodes, having two degrees of freedom at each node, having plasticity and large deflection strain capabilities. The BC used to obtain stress distributions can be seen in Figure 9. For the failure load and the load-displacement curves, the distributed load must be replaced by a BC of displacement, since the experimental tests are performed with a constant displacement rate.

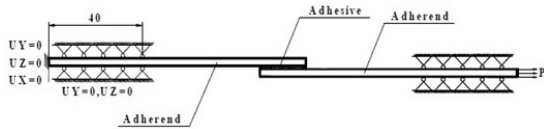


Figure 9: Boundary conditions of the SLJ [21].

Also, as stated in Subsection 2.2, the SLJ shall be modelled with the adhesive fillet, as well as with the rounded adherent corners. Two different geometries were then considered in this analysis: the normal SLJ (Geometry 1, or G1) and the SLJ modelled as previously stated (Geometry 2 or G2).

Using the Centerline Method, the stress distributions for G1 and G2 were obtained in Figure 10, highlighting the great reduction in in the maximum values of shear and peel stresses in both adhesives. This indicate that, in principle, the failure loads will be higher for G2.

Applying the PFM described in Subsection 2.2, the failure loads presented in Table 5 were obtained. These values must be used to validate the model.

With the results presented in Table 5, it is clear that Geometry 2 must be the one used to calculate the failure load of the SLJ. With relative errors of

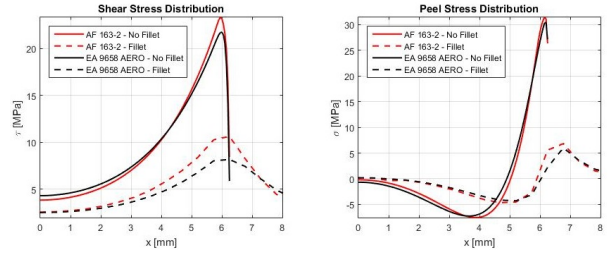


Figure 10: Stress distributions, obtained computationally for G1 and G2, using both adhesives.

Table 5: Failure loads obtained.

P_f [N]	AF 163-2		EA 9658	
	G1	G2	G1	G2
Datasheet	12281		12500	
PFM	5151	8971	6093	11142
Rel. Error [%]	58.06	26.95	51.26	10.86

26.95% and 10.86% for adhesives AF 163-2 and EA 9658 AERO respectively, the results are considered quite acceptable.

In Figure 11, the computational and experimental load-displacement curves, for the AF 163-2 adhesive, are compared. The differences between the curves are evident, being only similar for small displacements. This discrepancy may be explained by the fact that, since the applied surface treatments are not the advised, that the specimens presents some loss of adherence, presenting less resistance to loading than expected. If compared with the curve obtained for a SLJ treated with CAA [30] (green curve in Figure 11), it can be seen that the slopes are quite similar, which corroborates the hypothesis of adherence loss.

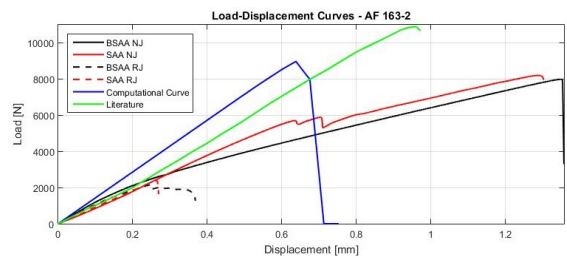


Figure 11: Comparison between load-displacement curves for the AF 163-2.

Finally, the failure of the SLJ is compared in Figure 12 and several resemblances can be found. Numbers 1 and 2 represents similar zones of the fracture. Zone 1 represents the location of the fillet when failure occurs. As it can be seen, the major part of the fillet stays bonded to the respective adherent, with the crack occurring near the overlap area. Zone 2 represents some adhesive that stays bonded in the face of the adherent, showing once

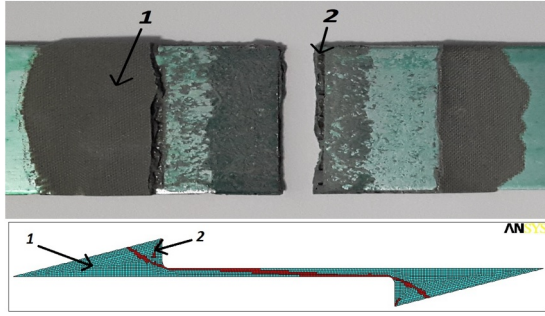


Figure 12: Comparison between experimental (on top) and computational (on bottom) failures for a EA 9658 AERO specimen.

again concordance between both results.

With all the results presented, one can conclude that the adhesive behavior, for the SLJ, has been reproduced computationally with a relatively good degree of accuracy.

5. Conclusions

Regarding the first objective, a new combination of adhesive and surface treatment, at least as good as the old one was found, has indeed been found. SAA NJ, bonded with AF 163-2, managed to achieve a result 8% better than the old combination. However, it presented a very poor behavior when applied to RJ, whereby the appliance of this adhesive in this type of joints can jeopardize the safety of the structure. Despite the improvement revealed by the EA 9658 AERO in RJ, it is not possible to guarantee the safety of this type of joints.

Said so, and even knowing that the results obtained by the ASTM D 1002 are quite significant, some other tests shall be performed to ensure the quality of the bonding. One must note that, despite being used in aluminum-to-aluminum joints, the adhesive chosen will also be applied in honeycomb sandwich panels, so the behavior of both AF 163-2 and EA 9658 AERO must also be tested in this type of structures.

Relatively to the second part of the work, it was completed with a good degree of success. Using just the stress-strain curve of both adhesives, it was possible to model the adhesive behavior. There were, however, some results that were not totally in accordance with the observations, specially the curves from the ASTM D 1002 test, which can be related with the use of different surface treatments from the ones advised by the manufacturers. This may cause a lower adherence between adhesive and substrates, compromising the curves that would be obtained for perfect adherence.

With this in mind, some more experimental tests should also be performed for validation. Firstly, the bulk test should be performed for both adhesives,

to obtain the correct mechanical properties of each. This would certainly help to a better and more accurate modulation of the adhesive layer. Plus, the ASTM D 1002 should be performed once again, this time with the respective advised surface treatments. Furthermore, the model must be applied to some other bonded structures. The ANSYS APDL code was developed in order to be applied to any bonded geometry, so this would be a very interesting study.

References

- [1] Robert D. Adams and William C. Wake. *Structural Adhesive Joints in Engineering*. Chapman and Hall, 2nd edition, 1997. ISBN:978-0-412-70920-3.
- [2] Jun Cui. Finite element modeling of adhesive failure with adherend yielding. Master's thesis, University of Toronto, 2001.
- [3] Ahmet Calik. Effect of adherend shape on stress concentration reduction of adhesively bonded single lap joint. *Engineering Review*, 36(1):29–34, January 2016.
- [4] Olaf Volkersen. Nietkraftverteilung in zugbeanspruchten nietverbindungen mit konstanten laschenquerschnitten. *Luftfahrtforschung*, pages 15–41, 1938.
- [5] Goland and Reissner. The stresses in cemented joints. *Journal of Applied Mechanics*, 11:A17–A27, March 1944.
- [6] L.I. John Hart-Smith. Adhesive-bonded single-lap joints. Technical Report NASA CR-112236, National Aeronautics and Space Administration, jan 1973.
- [7] L. F. M. da Silva and R. D. S. G. Campilho. Advances in numerical modelling of adhesive joints. *SpringerBriefs in Computational Mechanics*, 2012. DOI: 10.1007/978-3-642-23608.
- [8] Yinhan Yang. Stress analysis and failure prediction of adhesively bonded single-lap laminates joints subjected to the tensile loading. *IJSH International Journal of Smart Home*, 11:19–28, 2015.
- [9] R.D. Adams and R. Davies. *The Mechanics of Adhesion*, chapter Strength of lap shear joints. Elsevier, Amsterdam, 2002.
- [10] R.D. Adams and N.A. Peppiatt. Effects of poisson's ratio strains in adherend on stresses of an idealized lap joint. *The Journal of Strain Analysis for Engineering Design*, 8(2):134–139, April 1973. DOI: 10.1243/03093247V082134.

- [11] Tongyan Yue and M. Abdel Wahab. Finite element analysis of stress singularity in partial slip and gross sliding regimes in fretting wear. *Wear*, 321:53–63, December 2014. doi:10.1080/10618560701678647.
- [12] X. Zhao, R.D. Adams, and L.F.M. da Silva. Single lap joints with rounded adherend corners: Stress and strain analysis. *Journal of Adhesion Science and Technology*, 25(8):819–836, February 2011. DOI: 10.1163/016942410X520871.
- [13] D.C. Noorman. Cohesive zone modelling in adhesively bonded joints: Analysis on crack propagation in adhesives and adherends. Master’s thesis, Delft University of Technology, Sep 2014.
- [14] Mohammed Waseem H.S. and Kiran Kumar N. Finite element modeling for delamination analysis of double cantilever beam specimen. *International Journal of Mechanical Engineering*, 1(5):23–33, September 2014.
- [15] R. D. S. G. Campilho, M. D. Banea, A. M. G. Pinto, L. F. M. da Silva, and A M P de Jesus. Strength prediction of single - and double - lap joints by standard and extended finite element modelling. *International Journal of Adhesion & Adhesives*, 31:363–372, February 2011. doi:10.1080/10618560701678647.
- [16] Fiamegkou Ch. Eleni. Development of improved, multi-functional, nano-structured polymer based adhesives with applications in the bonding of composite components and the repair of engineering structures with composite patches. Master’s thesis, University of Patras, 2015.
- [17] Mahmood Shokrieh. Failure of laminated composite pinned connections. Master’s thesis, Iran University of Science and Technology, Jul 1991.
- [18] Michael Maletta. The development of a progressive failure model of a fiber-reinforced composite lamina. Master’s thesis, Grand Valley State University, Apr 2008.
- [19] Konstantinos N. Anyfantis and Nicholas G. Tsouvalis. Post buckling progressive failure analysis of composite laminated stiffened panels. *Applied Composite Materials*, February 2011. DOI 10.1007/s10443-011-9191-1.
- [20] Khudhayer J. Jadee. Progressive failure analysis and failure map into plain weave glass fibre reinforced polymer bolted joint. *American Journal of Materials Science and Engineering*, 3(2):21–28, 2015. DOI:10.12691/ajmse-3-2-1.
- [21] Yinhan Yang. Stress analysis and failure prediction of adhesively bonded single-lap laminates joints subjected to the tensile loading. *International Journal of Smart Home*, 9(11):19–28, 2016. ISSN: 1975-4094 IJSH.
- [22] John Tomblin, Waruna Seneviratne, Paulo Escobar, and Yap Yoon-Khian. Shear stress-strain data for structural adhesives. Final Report DOT/FAA/AR-02/97, Wichita State University, Wichita, KS 67260, Nov 2002.
- [23] D. S. Cobb, M. A. Vargas, T. A. Fridrich, and M. R. Bouschlicher. Metal surface treatment: Characterization and effect on composite-to-metal bond strength. *Operative Dentistry*, 25:427–433, 2000.
- [24] Austin Vaillancourt and Travis Abele. Adhesive technology: Surface preparation techniques on aluminum. Technical report, Worcester Polytechnic Institute, 2006.
- [25] Edward M. Petrie. *Handbook of Adhesives and Sealants*. The McGraw-Hill Companies, Inc., second edition, 2007. ISBN: 9780071479165.
- [26] ASTM Standards. *Standard Test Method for Apparent Shear Strength of Single-Lap-Joint Adhesively Bonded Metal Specimens by Tension Loading (metal-to-metal)*, Oct 1999.
- [27] Sofia Teixeira de Freitas and Jos Sinke. Temperature effect on the static behaviour of adhesively-bonded metal skin to composite stiffener. *ABCM International Congress of Mechanical Engineering*, 23, December 2015.
- [28] J. A. Harris and R. D. Adams. Strength prediction of bonded single lap joints by non-linear finite element methods. *International Journal of Adhesion and Adhesives*, 4(2):65–78, April 1984. DOI: 10.1016/0143-7496(84)90103-9.
- [29] A. D. Crocombe. Global yielding as failure criteria for bonded joints. *International Journal of Adhesion and Adhesives*, 9(3), 1989.
- [30] Miguel Pereira Palmares. Strength of hybrid laminates aluminium carbon-fibre joints with different lay-up configurations. Master’s thesis, Faculdade de Engenharia da Universidade do Porto, July 2016.